JOURNAL OF CATALYSIS 117, 237–245 (1989)

Infrared Spectroscopy and Redox Studies of Coexchanged Europium and Iron in Y-Zeolite

M. A. ULLA,*,[1] L. A. APARICIO,† J. A. DUMESIC,† AND W. S. MILLMAN*,[2]

*Department of Chemistry, University of Wisconsin, Milwaukee, Wisconsin 53201, and †Department of Chemical Engineering, University of Wisconsin, Madison, Wisconsin 53706

Received May 30, 1988; revised November 1, 1988

Carbon monoxide and nitric oxide chemisorption on europium-exchanged Y-zeolite and on Eu and Fe coexchanged Y-zeolite was studied using infrared spectroscopy. Redox studies were carried out gravimetrically to determine the extent of oxidation–reduction for the cations, the reactivity, and the average oxidation state under different ratios of oxidant and reductant. Eu–Y was found to reduce with difficulty whereas EuFe–Y underwent a more facile reduction, yet not as easily as Fe–Y. The EuFe–Y catalyst was found to operate at near its fully oxidized state under $CO:O_2$ ratios of 10 : 1. In contrast, the oxidation state of Fe–Y is dictated by the overall stoichiometry of the gas phase. For example, a 2 : 1 $CO:O_2$ ratio results in an average oxidation state of +2.5. The time dependence of the NO spectral areas upon exposure of reduced EuFe–Y to NO exhibits changes similar to those found for Fe–Y, except for the initial exposure. These data are consistent with Eu forcing Fe into sites of higher accessibility. This phenomenon has also been seen for Fe in Y-zeolites with silicon-to-aluminum ratios larger than 2.5. The time dependence of the infrared bands upon exposure to NO is consistent with migration of the Fe into new sites, as was found earlier for Fe–Y. © 1989 Academic Press, Inc.

INTRODUCTION

The effectiveness of a base exchange cation for carrying out redox reactions within a zeolytic framework has been shown to depend not only on the redox characteristics of the base exchange cation but also on the location of that cation within the zeolite framework and also on the nature of the framework itself. An illustration of the latter effect is provided by a comparison of Fe(II)-exchanged Y-zeolite with its Mordenite analog. The rates for the reaction of CO with NO over these catalysts are comparable, yet Mordenite contains about 16% of the amount of iron. Thus, on a per iron cation basis, Fe–Mordenite is a superior catalyst to Fe–Y zeolite (*1–3*). Similar comparisons have been made within the Y-zeolite structure. Modification of the silicon-to-aluminum ratio of the Y-zeolite by silicon substitution before iron exchange resulted in the expected loss of base exchange capacity. However, the effectiveness of the iron in carrying out the redox cycle for N_2O decomposition was significantly improved (*4*). The cause of the increased reactivity of iron has been shown to result from changes in the occupancy of the base exchange sites within the zeolite framework. As the silicon-to-aluminum ratio is increased the Fe cations move from predominantly site I into sites I′, II′ and/or II (*5*), or possibly III′ (*6*).

Modification of the cation location has been demonstrated not only by changing the silicon-to-aluminum ratio but more classically by coexchange with a second cation (*1*). The reactivity of zeolites coexchanged with a second cation has shown that the redox activity may be enhanced (*1*). Of various combinations reported earlier (*1*), that of Eu and Fe is particularly attractive because both nuclei lend themselves to examination by Mössbauer spectroscopy. Addi-

[1] On leave from INCAPE, Sante Fe, Argentina.

[2] To whom all correspondence should be addressed.

0021-9517/89 $3.00
Copyright © 1989 by Academic Press, Inc.
All rights of reproduction in any form reserved.

tionally, Eu–Y itself does not exhibit any catalytic activity for the reaction between CO and NO or N_2O decomposition.

We report in the present paper studies of the reversibility, catalytic activity, and cation locations in EuFe–Y-zeolite. These studies involved IR analysis of the chemisorption of NO together with microbalance characterization of the redox half-reactions where oxidation and reduction were carried out in O_2 and H_2 or CO, respectively.

EXPERIMENTAL

The Eu–Y and EuFe–Y samples were the same samples used in our earlier work (*1*). The preparation was described previously and the unit cell composition can be described as Eu–Y—Si_{142} Al_{50} Na_{12} Eu_{13} O_{384} (Eu/g = 5.7×10^{20}) and EuFe–Y—Si_{140} Al_{52} Na_9 Eu_8 Fe_{10} O_{384} (Eu/g = 3.58×10^{20}, Fe/g = 4.47×10^{20}).

Redox properties and rates of reduction and oxidation were studied using a Cahn Electrobalance (Model C-2000) operated in the flow mode. The detailed experimental conditions were the same as those previously described (*2, 3*).

A Nicolet Model MX-1 Fourier transform spectrometer equipped with a Model 620 data station was used to obtain infrared spectra. A vacuum-tight IR cell having KBr windows and a self-contained furnace was used for the experiments. This cell was attached to a flow system or standard vacuum system with provisions for measuring gas volumes. Samples were prepared as self-supporting wafers having a thickness of 5 to 7 mg/cm^2. These wafers were subsequently treated in various flowing gases (100 cm^3/min). The initial treatment involved heating at a rate of 5 K/min and holding at progressively higher temperatures of 373, 473, 573, 673, and 773 K for each measurement. The samples were kept under He flow (100 cm^3/min) until 573 K and then O_2 (25%) was added to the He. The samples were held at each of the above temperatures for 40 min and maintained at 773 K for 40 h. This process was carried out prior to each reduction.

Reduction was carried out in either CO or H_2 (25%) which was diluted in the He carrier gas. Additional experiments were carried out after the catalysts had been equilibrated at 773 K in a flowing 3 : 1 mixture of CO and O_2 diluted in He.

After each pretreatment, oxidation, reduction, or reaction, the IR cell was purged with flowing He for 5 min at 773 K and then cooled to room temperature and evacuated to 10^{-5} Torr. Infrared spectra were obtained at room temperature with the spectrometer operating in the absorbance mode.

The gas purification procedures used in this study have been described elsewhere (*4*).

Kinetic measurements for the oxidation of carbon monoxide were made using a continuous-flow, single-pass reactor. Fractional conversions were determined by mass spectral analysis of the effluent gas. The gas analysis procedure and the detailed experimental conditions have been described previously (*3*).

The rates of CO oxidation are expressed as the number of molecules of CO transformed into CO_2 per second per gram of catalyst. These were determined under differential reaction conditions from the initial slope of a plot of fractional conversion versus W/F, where W was the catalyst weight and F the flow rate of CO. Values of W/F ranged from 0.625 to 2.50 mg · min/cm^3. Activation energies were determined from four temperatures between 623 and 823 K.

The gas composition was 1.9% O_2 and 3.8% CO in all experiments, with He making up a total pressure of 1 atm.

RESULTS

Microbalance Redox Studies

The oxidation state of EuFe–Y and Eu–Y during oxidation and reduction cycles was studied gravimetrically by monitoring the weight of the samples after treatment with different redox couples, e.g., H_2/O_2,

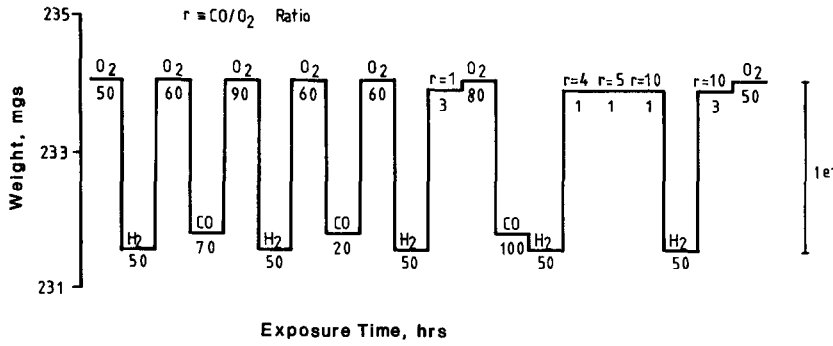

FIG. 1. Results of flow microbalance studies of EuFe–Y in oxidation–reduction cycles at 770 K. The gas flowing over the catalyst is identified above the equilibrium weights (taken in He to provide a constant basis with respect to buoyancy). r represents the CO/O_2 ratio. Values for treatment times (in hours) are given below the lines.

H_2/N_2O, and CO/O_2. The experiments were carried out at 773 K, and typical results are shown in Figs. 1 and 2. The data show that the catalysts were stable and could be reversibly oxidized and reduced over many cycles. Using H_2/O_2 and H_2/N_2O redox couples, the weight change measured for EuFe–Y showed that the amount of oxygen removed or added corresponded to an O/M atomic ratio of 0.49 (M = Fe + Eu), whereas with the CO/O_2 couple a ratio of O/M equal to 0.46 was obtained. For Eu–Y, a ratio of 0.80 O/Eu was measured for all three redox couples. This apparent reduction below an oxidation state of

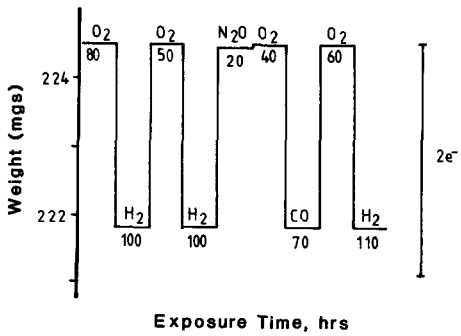

FIG. 2. Results of flow microbalance studies of Eu–Y in oxidation–reduction cycles at 770 K. The gas flowing over the catalyst is identified above the equilibrium weights (in He). Values for treatment times (in hours) are given below the lines.

Eu^{2+} is not consistent with the available information from the literature (*13, 14*) and is the subject of further studies. It should be noted that in Fe–Mordenite we also found an apparent reduction below Fe^{2+} with a CO/O_2 redox couple which was due to a water–gas shift reaction along with the reduction. This resulted in an additional weight loss due to the dehydroxylation beyond that found thermally (*12*).

The weight of the EuFe–Y sample under reaction conditions for CO oxidation was also monitored. The results are shown in Fig. 1. Five reactant gas ratios were used in these experiments. These were CO/O_2 ratios (r) equal to 1, 3, 4, 5, and 10. The weights of the oxidized and reduced states obtained when O_2, CO, or H_2 was the only reacting gas were used for comparison. Under CO oxidation conditions, the weight of the catalyst was close to that of the fully oxidized state, even when the feedstream was strongly reducing overall (e.g., $r = 10$). The same steady-state weight was obtained when the reaction was started from either the oxidized or the reduced state. This behavior is in contrast to results for Fe–Y (2), where the weight of the catalyst reflected the CO/O_2 ratio. For example, with a CO/O_2 ratio of 2, the catalyst weight indicated the Fe had an average oxidation state of 2.5. In EuFe–Y the average metal oxida-

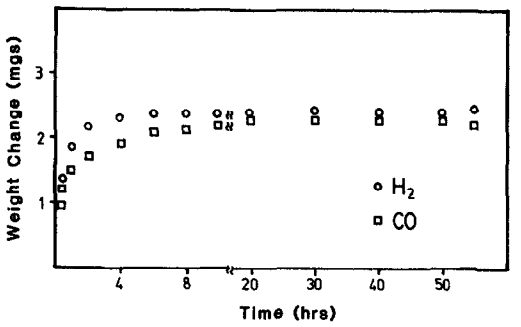

FIG. 3. Plots of weight change as a function of time for oxidized EuFe–Y during the reduction in H_2 and CO. The last open points, at the end of the plot, are the weights on a constant basis in He to correct for buoyancy differences.

tion state is 2.88. Whether Eu or Fe is being reduced under these conditions is addressed below.

Figures 3 and 4 show the sample weight versus time during oxidation and reduction of EuFe–Y. It can be seen that the oxidation and reduction processes appear to have two regimes. An initial fast step occurs over about 1 h, during which 60–85% of the total weight change takes place. The second step required much longer times for the sample to reach its final weight. It should be noted that just 60% of the total weight change occurred during the first step when CO was the reducing agent. In contrast, 80% of the total weight change occurred during the first step when H_2 was the reducing agent. The overall reduction rate of the Eu–Y zeolite was found to be much slower than that for the reduction of EuFe–Y. In work to be published soon, we show another difference between the two zeolites: the reduction of EuFe–Y is faster when H_2 is the reducing agent, whereas the reduction of Eu–Y is faster when CO is the reducing agent. Evidence for this is the rate of weight change in the microbalance under flow conditions with 10% reducing agent diluted in He.

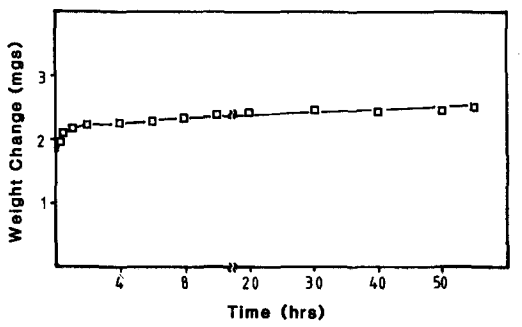

FIG. 4. Plot of weight change as a function of time for reduced EuFe–Y for oxidation with O_2. The last point, at the end of the plot, is the weight on a constant buoyancy basis using He.

Infrared Spectroscopy

An oxidized EuFe–Y sample was reduced in flowing H_2 at 773 K for 50 h and then purged with flowing He for 5 min at the same temperature. The cell was subsequently cooled to room temperature, evacuated to 10^{-5} Torr, and filled to 3 Torr with NO. Figures 5A–C show the IR spectra obtained after exposure of the sample to NO for 15 s, 10 min, and 24 h, respectively. The 15-s exposure was followed by a 1-h evacuation. The spectra exhibited bands at 1920, 1884, 1853, and 1817 cm^{-1}, with the bands

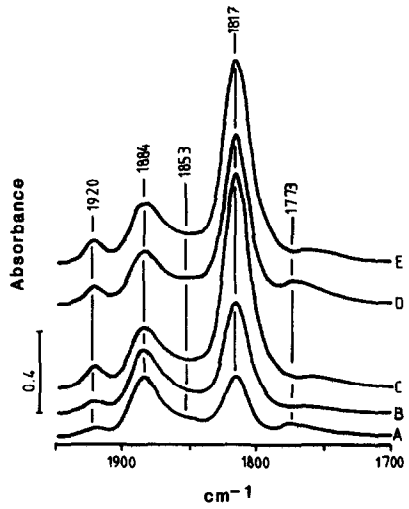

FIG. 5. Infrared spectra of EuFe–Y reduced with H_2 for 50 h after different treatments: (A) 400 Pa of NO for 15 s and evacuated for 1 h; (B) 400 Pa of NO for 10 min; (C) 400 Pa of NO for 24 h; (D) after 1 h evacuation; (E) after reexposure to 400 Pa of NO for 10 min.

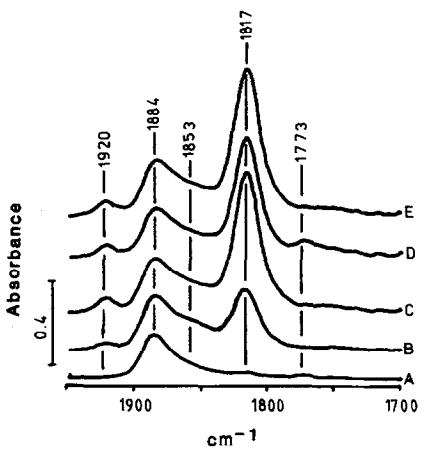

FIG. 6. Infrared spectra of EuFe–Y reduced with CO for 50 h after different treatments: (A) 400 Pa of NO for 15 s and evacuation for 1 h; (B) 400 Pa of NO for 10 min; (C) 400 Pa of NO for 24 h; (D) after 1 h evacuation; (E) after reexposure to 400 Pa of NO for 10 min.

at 1920 and 1817 growing slowly with exposure. Evacuation of the sample following exposure to NO for 24 h caused a decrease in the bands at 1920, 1884, and 1817 cm^{-1} and the growth of a new band at 1773 cm^{-1} (Fig. 5D). Reexposure of this sample to NO resulted in the spectrum shown in Fig. 5E, which is identical to that obtained after initial exposure for 24 h.

Figure 6 shows spectra obtained using a procedure identical to that used to obtain the spectra shown in Fig. 5, except that reduction was carried out using CO. The spectrum in Fig. 6A was recorded after 3 Torr of NO was introduced for 15 s, after which the cell was evacuated for 1 h. The data show that the 1884 and 1854 cm^{-1} bands appear immediately. These observations are identical to those following hydrogen reduction. However, the bands at 1920 and 1817 cm^{-1} were not present initially. This suggests that the sites available for NO adsorption depend on which reducing agent is used. The spectra for the CO reduced sample (Figs. 6B–E) are similar to those found following reduction in H_2, i.e., the 1920, 1884, 1854, and 1817 cm^{-1} bands appear at similar rates. Finally, as with H_2 reduction, the 1773 cm^{-1} band was present only after evacuation.

To examine in more detail the difference between reducing with H_2 and CO, EuFe–Y was reduced under three different conditions: (1) with H_2 for 1 h, (2) with CO for 1 h, and (3) with H_2 for 1 h followed by CO for 1 h. All these experiments were preceded by the standard oxidation treatment, as outlined above. Identical NO adsorption experiments were carried out after each of these pretreatments. The IR spectra of NO adsorbed on samples reduced in H_2 for 1 h were similar to those obtained on the samples following reduction in H_2 for 50 h, with the exception that the total spectral area was slightly lower in the former case. Most important are the spectra in Fig. 7 which are for a sample reduced in H_2 followed immediately by reduction in CO. These spectra are similar to those obtained on a sample after reduction for 1 h in CO alone. Furthermore, these spectra show the same low intensity of the bands at 1920 and 1817 cm^{-1} characteristic of the sample reduced in CO for 50 h. Thus, CO reduction of a H_2 prereduced sample changes the cation sites for NO adsorption from that present after the hydrogen reduction to that present after a CO reduction.

Analogous experiments were carried out on a Eu–Y sample that had been reduced

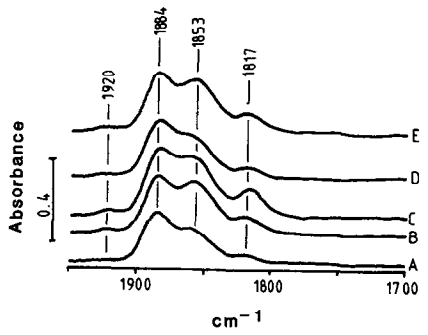

FIG. 7. Infrared spectra of EuFe–Y reduced with H_2 for 1 h followed by CO for 1 h after different treatments: (A) 400 Pa of NO for 15 s and evacuation for 1 h; (B) 400 Pa of NO for 10 min; (C) 400 Pa of NO for 24 h; (D) after 1 h evacuation; (E) after reexposure to 400 Pa of NO for 10 min.

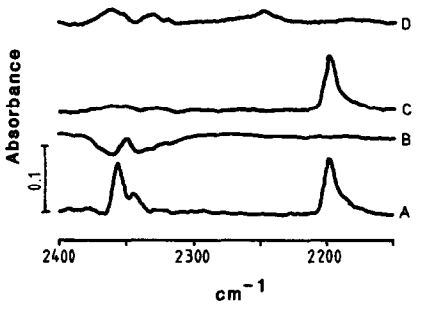

FIG. 8. Infrared spectra of EuFe–Y following various treatments: (A) after reduction with CO; (B) reduced with CO followed by 400 Pa of NO for 15 s and evacuated for 1 h; (C) reduction in H_2 followed by exposure to 4000 Pa of CO; (D) after 4000 Pa of NO.

with CO for 100 h. Microbalance data showed a 1.6-electron reduction of Eu under these conditions. In this case, IR spectroscopy showed that the extent of NO adsorption was negligible. These results provide an indication that Fe alone was responsible for the formation of the nitrosyl complexes seen above.

The interaction between carbon monoxide and the EuFe–Y sample was also studied by infrared spectroscopy. The spectrum of this sample after reduction with CO (Fig. 8A), shows three bands at 2356, 2345, and 2190 cm^{-1}. The band near 2345 cm^{-1} is attributed to adsorbed CO_2, whereas the band at 2356 cm^{-1} is associated with a direct interaction of CO_2 with the cation by an ion-dipolar interaction (*7, 8*) as shown:

$$M^{n+} \cdots O^{\delta-} = C = O^{\delta+}.$$

The 2190 cm^{-1} band can be assigned to CO interacting directly with the cation (*9*). Upon exposure to NO the CO_2 and CO peaks in the spectrum disappeared (Fig. 8B). This suggests that nitric oxide efficiently displaces both CO_2 species and CO adsorbed on exchanged iron cations.

Carbon monoxide adsorption on a EuFe–Y sample reduced with H_2 for 1 h was also studied by IR spectroscopy. The sample was exposed to 30 Torr of CO and the resulting spectrum is shown in Fig. 8C. The spectrum has one peak at 2190 cm^{-1} attributable to a cation–CO interaction. The IR cell was then filled with 30 Torr of NO and the spectrum shown in Fig. 8D was obtained. The latter spectrum shows complete removal of CO in a manner identical to that for the CO reduced sample above. It is therefore concluded that when reduced EuFe–Y is exposed to CO and NO no mixed complexes such as CO–M–NO are formed. This observation is at variance with the findings of Kasai *et al.* over activated Ni–Mordenite (*10*). The features near 2350 cm^{-1} in Figs. 8B and D are due to imperfect subtraction of gaseous CO_2 in the spectrometer.

Additional experiments involving NO adsorption were carried out on oxidized EuFe–Y and after the oxidized EuFe–Y had reached steady state for CO oxidation at 773 K in a flowing gas mixture (CO/O_2 = 3). The results are given in Fig. 9. Figures 9A and B were obtained after NO exposure of samples of EuFe–Y that had been reduced in H_2 and CO, respectively. Figure 9C shows the spectrum of the sample exposed to NO after carrying out the CO oxidation reaction; Fig. 9D was obtained after NO exposure of an oxidized EuFe–Y sample. Figure 9D shows that NO adsorption on Fe^{3+} is negligible, in agreement with the observations of Segawa *et al.* (*5*). The low spectral intensity of Fig. 9C compared with Figs. 9A and B shows that EuFe–Y is

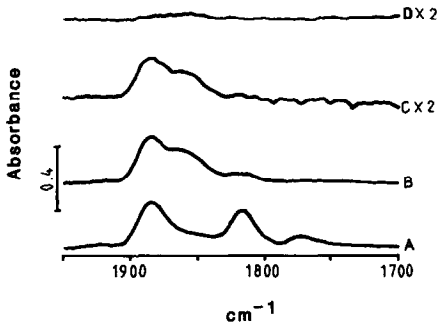

FIG. 9. NO infrared spectra on EuFe–Y: (A) reduced with H_2 for 1 h; (B) reduced with CO for 1 h; (C) after reaching steady-state reaction conditions in a flowing CO/O_2 gas mixture (CO/O_2 = 3); (D) oxidized.

TABLE 1

Catalytic Activity Comparison

Catalyst	Reactions				
	$CO + \frac{1}{2}O_2$[a]			$CO + NO$[b] TOF[d] (620 K)	N_2O decomposition[c] TOF[d] (700 K)
	Temperature range (K)	E_a (kcal/mol)	TOF[d] (620 K)		
EuFe–Y	350–550	12	141	96[f]	508[f]
Fe–Y	200–412	21[e]	282[e]	30[f]	57[f]
Fe–M	200–412	13[e]	487[e]	284[e]	822
Eu–Y	350–550	NR	NR	NR	NR

[a] Gas composition: 3.8% CO and 1.9% O_2, balance He.
[b] Gas composition: 3.0% CO and 6.0% NO, balance He.
[c] Gas composition: 7.0% N_2O, balance He.
[d] TOF: $\times 10^5$ molecules per Fe per second.
[e] Data from Ref. (*12*).
[f] Data from Ref. (*1*).

nearly fully oxidized under reaction conditions, even though the reactant gas ratio (CO/O_2) in this experiment was 3. This behavior is in agreement with the microbalance results (Fig. 1).

Finally, IR spectra in the CO region of Eu–Y and EuFe–Y after the catalysts had reached steady state (as described above) showed CO_2 bands at 2356 and 2350 cm^{-1} on both of the exchanged zeolites and the absence of bands attributable to CO.

Catalytic Behavior

The CO oxidation activity of Eu–Y and EuFe–Y zeolites was studied under stoichiometric reaction conditions. The data are presented in Table 1. For comparison, results obtained under identical experimental conditions for Fe–Y and Fe–Mordenite (Fe–M) (*2*) are given. In addition to data for CO oxidation with O_2, data for N_2O decomposition and CO oxidation with NO are included. These data shown that Eu–Y has no activity for any of these reactions. In contrast, the EuFe–Y sample was found to have a lower activation energy then Fe–Y, and a value similar to that of Fe–M. However, the activity per iron cation of the former zeolite is lower than that for the other samples. Interestingly the results obtained for the oxidation of CO by NO and for the N_2O decomposition showed EuFe–Y and Fe–M to be significantly more active than Fe–Y per iron cation.

The most significant differences between Fe–Y and EuFe–Y which may contribute to the different activity of the latter are (a) accessibility of the Fe to reactant gases and (b) the chemical environment of the Fe due to the effect of the ligand field in altering the energy required to oxidize the cation.

DISCUSSION

Chemical Environment

The reduction of Eu^{3+} in Eu–Y required at least 60 h to complete with CO, whereas 30 h was needed with H_2. In contrast, the reduction of EuFe–Y is complete, forming Eu^{2+} and Fe^{2+}, after less than 15 h in H_2. In addition, Fe–Y needs only 1 h for complete reduction or oxidation (*2*). Therefore the reduction rates in H_2 of the cations incorporated into the zeolites decreased in the order Fe–Y > EuFe–Y > Eu–Y.

Aparicio *et al.* (*1*) used Mössbauer spectroscopy to show that Eu in EuFe–Y is more easily reduced than Eu in Eu–Y. It can be deduced from those results and the microbalance results of the present study that the iron cations in EuFe–Y enhance the rate of reduction of Eu, whereas the Eu inhibits the reduction rate of the Fe^{3+} cations. Also in agreement with the effects of Eu on the redox properties of Fe in the coexchanged zeolite is the observation that the EuFe–Y catalyst operated in a nearly completely oxidized state, even at CO/O_2 ratios as high as 10. In contrast, Fe–Y and Fe–M catalysts, under the same conditions, operate in nearly the fully reduced state (*2*). The weak NO adsorption on EuFe–Y after the sample reached steady-state reaction conditions in a flowing CO/O_2 gas mixture (CO/O_2 = 3) at 773 K and the strong interaction with CO_2 during the reaction (Figs. 9C and 8A) are consistent with the above interpretation.

The presence of Eu in EuFe–Y may modify the chemical environment of Fe due to the effect of the ligand field, altering the lability of the oxygen that participates in the redox process. One simple means by which this modification may take place is through the formation of Fe–O–Eu bridges.

Location of Iron Cations

Previous infrared and Mössbauer spectroscopy studies of the interaction of NO with Fe-exchanged zeolites (*5*, *6*) assigned the infrared bands near 1845 and 1870 cm^{-1} to Fe^{2+} cation of low coordination which were accessible to gases (at site II and II′) and formed mononitrosyl complexes. The bands at 1920 and 1817 cm^{-1} were attributed to dinitrosyl complexes at site III′. The highly accessible iron cations associated with the dinitrosyl species are formed by migration of Fe^{2+} cation from sites of high coordination (presumably site I) which are energetically more favorable in the absence of NO. The appearance of a 1767 cm^{-1} band upon evacuation (Figs. 5D and 6D) is due to the dinitrosyl species at site III′ being converted into a mononitrosyl species.

When EuFe–Y was reduced with H_2 for 50 h, the mononitrosyl bands at 1880 and 1854 cm^{-1} and the dinitrosyl band at 1817 cm^{-1} appeared after the first exposure to NO. This suggests that sterically hindered cations (site II′), cations of intermediate accessibility (site II), and highly accessible cation (site III′) are already present prior to exposure to NO. In contrast, when the sample was reduced with CO for the same time, only a dominant band near 1884 cm^{-1} (site II′) was initially present. However, it is also clear that the samples had cations in sites of high coordination after the reduction with either H_2 or CO. Specifically, these cations migrate to locations of higher accessibility during the exposure to NO, since the bands at 1920 and 1817 cm^{-1} grew over a period of hours.

The IR spectra of this study show that the behavior of the EuFe–Y sample reduced with H_2 for 50 h is similar to that following reduction for 1 h, since the same bands appeared after NO adsorption; however, the intensity of the peaks generally increased with reduction time. These results agree with the microbalance results which indicated it was necessary to reduce for at least 15 h to complete the process: $M^{+3} \rightarrow M^{2+}$ (M = Fe + Eu). Also, the ratio of the intensities of the band at 1880 cm^{-1} to that at 1817 cm^{-1} was higher for the sample reduced in H_2 for 1 h than that reduced for 50 h. Since the 1817 cm^{-1} band is due to NO adsorption on cations at site III′ in the supercage, this could suggest that these cations migrate to a location of high accessibility during the reduction in H_2. This migration is apparently even more favorable upon reduction in CO.

Aparicio *et al.* (*1*) reported that EuFe–Y had a smaller fraction of ferrous cations at site I than conventional Fe–Y. In the present study it was also found that these cations are located at different sites after reduction of the EuFe–Y with H_2 or CO. When cations lose their extra-framework li-

gands during pretreatment, they tend to migrate to sites of high coordination (site I); therefore, Eu and Fe compete for these sites. When the sample was reduced with H_2, some of the ferrous cations were at site III′. The question then is why was Fe^{2+} in the EuFe–Y located at this site of high accessibility? The answer could be that Eu tends to occupy site I, thereby inducing Fe to populate other, more accessible sites (such as site III′). The observation that the infrared spectral features were different for EuFe–Y reduced with CO for 1 and 50 h (Figs. 6 and 9B) suggests that ferrous cations migrated during the reaction to sites in the zeolite that were energetically more favorable.

Additional support for the migration of cations in the presence of CO can be found in the IR spectra of NO adsorbed on EuFe–Y which has been reduced with H_2 and then with CO. After the first reduction, some of the iron cations were at site III′ (1920 and 1817 cm^{-1} bands), but subsequent reduction with CO moved these cations to sites II and II′ (1854 and 1884 cm^{-1} bands, respectively). Adsorbed CO_2 and CO are present in EuFe–Y after reduction with CO. This would stabilize, for example, the Eu cations in site II and allow the Fe cations to migrate to site I. Such behavior would explain the apparent differential weight when this zeolite was treated with H_2 or CO. The microbalance results show that the weight after reduction in CO is larger than with H_2.

CONCLUDING REMARKS

Two models have been proposed to described the oxygen-carrying capacity of Fe–Y. In one model, it was suggested that Fe–O–Fe bridges formed upon oxidation (*11*), whereas in a later model it was proposed that a single Fe^{3+} cation in site III′ could hold an oxygen atom, with one electron being supplied by a second Fe cation (*5*). Regardless of which model is adopted, the observation that one oxygen atom is held for every two iron cations in conventional Fe–Y suggests that the oxidation process may require pairs of iron cations in close proximity. When Eu^{3+} is coexchanged with iron in Y-zeolite, the Fe can also have Eu as its near neighbor. It is therefore possible that the oxygen is adsorbed, in part, on Eu–Fe pairs. This model is supported by the results obtained from microbalance measurements, IR and Mössbauer spectroscopy, and catalytic studies (*1*). It is clear from these data that the Eu in EuFe–Y modifies the location and the chemical environment of the iron. The most striking modification is that iron is forced from site I into more accessible sites. This same effect was observed earlier by increasing the Si/Al ratio of the Y-zeolite (*4*, *6*).

ACKNOWLEDGMENT

The authors express their gratitude to the National Science Foundation for Grant CBT-8414622 which supported this work.

REFERENCES

1. Aparicio, L. M., Ulla, M. A., Millman, W. S., and Dumesic, J. A., *J. Catal.* **110,** 330 (1988).
2. Petunchi J. O., and Hall, W. K., *J. Catal.* **78,** 327 (1982).
3. Fu, C. M., Deeba, M., and Hall, W. K., *Ind. Eng. Chem. Prod. Res. Dev.* **19,** 299 (1980).
4. Aparicio, L. M., Dumesic, J. A., Fang, S. M., Long, M. A., Ulla, M. A., Millman, W. S., and Hall, W. K., *J. Catal.* **104,** 381 (1987).
5. Segawa, K., Chen, Y., Kubsh, J. E., Delgass, W. N., Dumesic, J. A., and Hall, W. K., *J. Catal.* **76,** 112 (1982).
6. Aparicio, L. M., Hall, W. K., Fang, S. M., Ulla, M. A., Millman, W. S., and Dumesic, J. A., *J. Catal.* **108,** 233 (1987).
7. Ward, J. W., *Zeolite Chem. Catal.* (*ACS Monogr.*) **171,** 118 (1976).
8. Angell, C. L., *J. Phys. Chem.* **70,** 2420 (1966).
9. Angell, C. L., and Schaffer, P. C., *J. Phys. Chem.* **70,** 1413 (1966).
10. Kasai, P. H., Bishop, R. J., Jr., and McLeod, D., Jr., *J. Phys. Chem.* **82,** 279 (1978).
11. Garten, R. L., Delgass, W. N., and Bourdart, M., *J. Catal.* **18,** 90 (1970).
12. Fang, S. M., Petunchi, J., Leglise, J., Millman, W. S., and Hall, W. K., *J. Catal.* **96,** 182 (1985).
13. Samuel, E. A. and Delgass, W. N., *J. Chem. Phys.* **62,** 1590 (1975).
14. Suib, S.L., Zerger, R. P., Stucky, G. D., Emberson, R. M., Debrunner, P. G., and Iton, L. E., *Inorg. Chem.* **19,** 1858 (1980).